ChemComm

View Online
Dynamic Article Links

Cite this: *Chem. Commun.*, 2011, **47**, 3903–3905

www.rsc.org/chemcomm

COMMUNICATION

Experimental demonstration of surface selection rules for SERS on flat metallic surfaces†‡

E. C. Le Ru,*[a] S. A. Meyer,[a] C. Artur,[a] P. G. Etchegoin,[a] J. Grand,[b] P. Lang[b] and F. Maurel[b]

Received 25th January 2011, Accepted 3rd February 2011
DOI: 10.1039/c1cc10484e

We have measured the polarization and incident angle dependence of the Surface-Enhanced Raman Scattering (SERS) signal of a nile blue monolayer adsorbed on a flat gold surface. Comparisons with predictions of electromagnetic (EM) theory indicate that the molecules are predominantly adsorbed flat on the surface. These results provide the most direct demonstration of the concept of surface selection rules in SERS, and further confirm the validity of the SERS-EM model beyond the $|E|^4$-approximation.

Surface-Enhanced Raman Spectroscopy (SERS)[1,2] is a unique characterization tool for molecules on metal surfaces. The determination of molecular orientation with SERS has been a longstanding goal.[3,4] For a fixed orientation on a metallic surface, the exact SERS intensity of each Raman mode depends on its tensor symmetry with respect to the surface, *i.e.* its orientation. Two main difficulties arise: (i) the knowledge of the Raman tensors of different modes, and (ii) the knowledge of the local field polarization at the molecule, and its connection with the SERS enhancement factor (EF). The Raman tensors can be obtained for small molecules by symmetry analysis or density functional theory (DFT). However, some may be modified upon adsorption (for instance in chemisorbed molecules, which are precisely the most likely to have a fixed orientation). The theoretical basis for the local field polarization was laid out by Moskovits,[5] who introduced the concept of Surface Selection Rules (SSRs) and studied the case of planar metallic surfaces in detail. The concepts were also extended to the case of a dimer of two metallic spheres;[6] a typical situation for SERS. SSRs also play an important role in interpreting some experiments probing the SERS chemical enhancement.[7]

Most experimental studies of SSRs have been performed in colloidal solutions,[8,9] where signal strength is not an issue but interpretations of molecular orientation are troublesome. In fact, they are purely based on the qualitative assumption that the local field polarization is primarily perpendicular ($\perp$) to the metallic surface. Hence, modes with a strong Raman tensor component normal to the surface are more enhanced than those with weak (or nil) normal components. By comparing the SERS EF of the various modes, and relating these to their bare Raman tensors, the molecular orientation can be partly inferred (in particular, whether the molecule sits flat or upright on the surface). Assuming the molecule has a well-defined adsorption orientation with respect to the surface, a number of conditions are required for such an approach to work: (i) The local field polarization must be predominantly $\perp$ to the surface: in particular at positions with the highest enhancements (there is no guarantee for this in complex substrates). (ii) The molecule must have several Raman modes with very different symmetries. The CH-stretch of small aromatic molecules can, for example, satisfy these conditions.[9] However, this typically prevents the study of resonant molecules like dyes (very common in SERS), since all the tensors in resonant Raman conditions have typically the same symmetry (imposed by the resonant electronic transition). (iii) The variations of the SERS EF across modes must be large enough to be distinguished from other effects. Among them, the unavoidable presence of plasmon resonance dispersion which introduces a Raman-shift dependence of the enhancements.[10,11] (iv) The SERS EF of each mode must be measurable since the important parameter is the relative SERS EFs of the various modes, not their relative SERS intensities. The need to know the non-SERS spectrum for this step again prevents the use of resonant molecules (like dyes).

These limitations provide the motivation to revisit the possibility of measuring SSRs on flat metallic surfaces, as presented in this communication. Provided there is no roughness, flat surfaces bestow the ultimate uniformity for SERS. Moreover, by changing the incident angle (θ) and polarization, we can modify the various components of the local field on the surface, thereby providing much richer information about tensor components. This lifts most of the limitations mentioned above, and leaves us with the "easier" problem of relating the Raman tensor to molecular orientation. The main disadvantage is that flat metallic surfaces have predicted SERS EF in the range $\sim$0–3 (we are therefore dealing with a surface Raman effect, with limited enhancement, but will nevertheless

[a] *The MacDiarmid Institute for Advanced Materials and Nanotechnology, School of Chemical and Physical Sciences, Victoria University of Wellington, PO Box 600, Wellington, New Zealand. E-mail: eric.leru@vuw.ac.nz*
[b] *Laboratoire ITODYS, Université Paris Diderot, CNRS - UMR 7086, 15 rue Jean de Baïf, 75205 Paris Cedex, France*

† This article is part of a ChemComm web-based themed issue on Surface Enhanced Raman Spectroscopy

‡ Electronic supplementary information (ESI) available. See DOI: 10.1039/c1cc10484e

retain the term SERS for simplicity). Thus SERS experiments become challenging with the concomitant low signals. Despite this, we demonstrate SSRs on a flat Au film (no roughness), *i.e.* in the spirit of the original proposal.[5] To compensate for low SERS EFs, we use a resonant analyte: Nile Blue at 633 nm excitation. The molecular orientation is inferred by SERS measurements as a function of incident angle and both incident and emitted polarizations. Results can be interpreted in the framework of Fresnel coefficients[5] and are further confirmed by an independent measurement using Polarization Modulation Infrared Reflection-Absorption Spectroscopy (PM-IRRAS).[12] The advantage of our approach here is that it is self-normalizing and thus avoids several limitations: (i) it does not require the SERS EFs (even relative EFs among modes), and is therefore not affected by modifications of the tensors upon adsorption, (ii) it does not require modes with different symmetries, thus allowing the study of resonant molecules, and (iii) it is not influenced by the plasmon resonance dispersion.[10,11] The advantages, however, do not come without limitations, which we will discuss.

Nile Blue was deposited on 45 nm Au films on glass (see Sec. S.I of the ESI‡). Samples were mounted on a rotation stage and measured in a backscattering geometry, as shown schematically in Fig. 1(a). To maximize the collected signal, it is desirable to use a high numerical aperture (NA) objective. However, a high NA objective presents several disadvantages: (i) it results in a spread of incident angles. (ii) The small spot size increases photobleaching, and prevents long integration times. (iii) It is challenging to focus on the surface at large angles. As a compromise, we used a × 20 (NA = 0.35) objective. The first two issues were eliminated by using an additional lens (focal length 500 mm) to focus the laser beam onto the back focal plane of the objective (Fig. 1(a)), resulting in a larger spot (≈35 μm diameter, instead of ≈5 μm) with negligible beam divergence. We measured the SERS intensity of the 590 cm^{-1} mode of NB as a function of θ for the four possible combinations of incident and detection polarizations (each being either Transverse Magnetic, TM, or Transverse Electric, TE; for example TE-TM will denote the "incident TE/detection TM" configuration). It may seem surprising at first that a SERS spectrum like the example shown in Fig. 1(b) can be obtained from a monolayer of molecules adsorbed on a flat Au film. A simple semi-quantitative estimate in fact gives a SERS EF of $F \approx 0.1$ for this measurement (see Sec. S.II of ESI‡), showing that it is indeed possible to observe a monolayer of dye with no enhancement (quenching in this case). In fact, since this SERS EF is in agreement with EM predictions, this also provides a direct experimental proof that roughness does not contribute here to the SERS signal (it would otherwise result in a much larger SERS EF).

The simplicity of the substrate allows the angular dependence of the SERS signal to be modeled accurately.[5,13] We calculated the electric field and SERS intensities at the air/gold interface for a multilayer system of air/Au (45 nm)/titanium (2 nm)/glass, which corresponds to our sample. The SERS EFs are here exact, *i.e.* they do not rely on the $|E^4|$ approximation, but use the optical reciprocity theorem[14,15] to take into account polarization effects[16] and the Raman tensor of the modes (details provided in Sec. S.III of the ESI‡). Since the beam divergence is negligible in our optical setup, the angle of incidence is well defined. For more accurate predictions we considered the effect of the NA for collection, by integrating the predicted intensities over a finite solid angle (see Sec. S.III‡). The only free parameters here are the components of the Raman tensor for the adsorbed molecules. It is instructive to consider the two extreme cases of a uniaxial tensor either ⊥ or ∥ to the surface (with orientation averaging in the latter case). Theoretical predictions are summarized in Fig. 2. The most important aspect is that the SERS signal associated with ⊥ components of the uniaxial Raman tensor (α_{zz}) clearly dominates (by a factor of ∼100) the signal in TM-TM configuration, but is absent from the other three (TM-TE, TE-TM, and TE-TE) which are dominated by in-plane components. Its angular dependence is also very different to the other ones, going from zero at $\theta = 0$ to a maximum around $\theta \sim 60°$. A measurement of the TM-TM signal and of one of the other three configurations should therefore provide a clear indication of the importance of perpendicular components relative to in-plane ones.

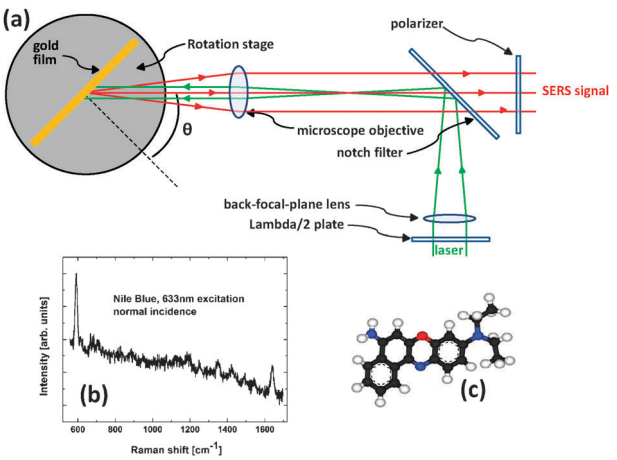

Fig. 1 (a) Schematics of the experimental setup. (b) Representative SERS spectrum of Nile Blue (shown in c), obtained at normal incidence, in TE-TE configuration, integration time 10 s.

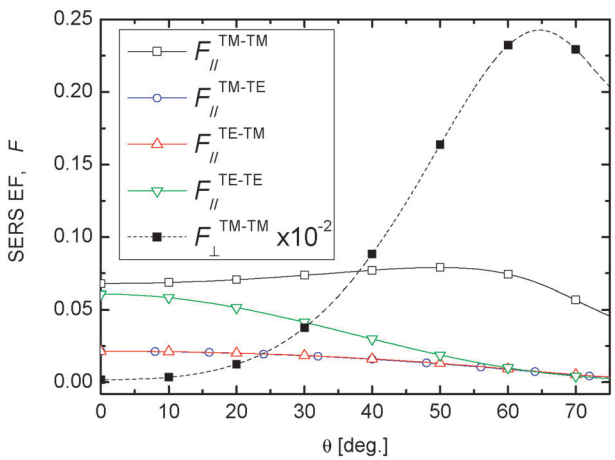

Fig. 2 Predictions for the angle- and polarization dependence of the SERS signal assuming a uniaxial Raman tensor with main axis either ⊥ or ∥ (with orientation averaging) to the Au surface.

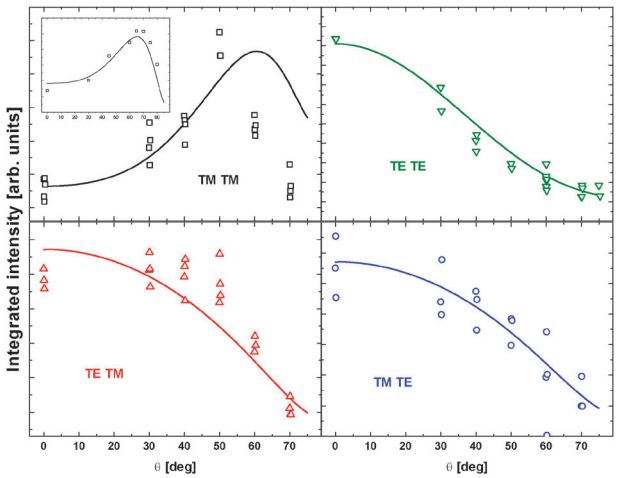

Fig. 3 Angle-dependence of the integrated SERS intensity for the 4 polarization configurations using a × 20 NA = 0.35 objective. Several positions on the sample were measured for each θ. Solid lines are the theoretical predictions (see Sec. S.III for details‡), assuming for TM-TM a contribution of 0.3% of $\perp$ components. At large θ's, the ×20 objective becomes inaccurate; its depth of focus limits the collected signal. The inset in (a) shows the data and predictions for TM-TM using a × 4 NA = 0.1 objective.

The experimental data for the angle- and polarization-dependent SERS signal are shown in Fig. 3. The TE-TE, TM-TE, and TE-TM signals are only sensitive to $\parallel$ tensor components and follow well the corresponding predictions. The TM-TM dependence exhibit a maximum at large θ's, but not as pronounced as predicted for a $\perp$ uniaxial tensor. To be more quantitative, the data for the TM-TM configuration can be fitted with a linear superposition of the $\perp$ and $\parallel$ predictions as shown explicitly in Fig. 3. A fraction of only 0.3% is derived for the $\perp$ component. For NB at 633 nm excitation, Raman tensors are expected to pick up the symmetry of the electronic state responsible for the absorption. Hence, they will have their components in the plane of the four conjugated rings of the molecule, and will (most likely) be uniaxial in this plane. We conclude that the NB molecules adsorb *flat* on Au; a fact expected for aromatic molecules. The small observed contribution of out-of-plane components (0.3%) is either due to minute sample imperfections resulting in the occasional molecule standing upright (or with a tilt) on the surface, or to a slight deviation from a perfectly planar adsorption geometry. Similar results were obtained for the 1645 cm^{-1} mode (see Fig. S5 of the ESI‡). This confirms that both modes have the same Raman tensor symmetry, as expected here. The adsorption orientation was independently confirmed from a comparison of IR absorption and PM-IRRAS[12] to the predictions of DFT (see Sec. S V of the ESI‡). Most of the IR modes that appear in the PM-IRRAS spectrum can be attributed (using DFT) to out-of-plane IR dipoles, in particular the CH bending modes around 800 cm^{-1}. This confirms independently the flat adsorption geometry, and therefore the SSRs/SERS analysis.

In closing, we have provided an experimental demonstration of SSRs in SERS in arguably the simplest possible case and along the very lines of the original proposal (almost thirty years ago).[5] Moreover, we highlight the possibility of measuring SERS from a monolayer of dye even in the absence of any enhancement. Our results provide a textbook-like confirmation of the validity of the EM model for SERS beyond the $|E|^4$-approximation, including polarization and orientation effects.

ECLR acknowledges support from a Marsden grant and a Rutherford discovery fellowship. SAM would like to thank Rose A. for her support.

References

1 E. C. Le Ru and P. G. Etchegoin, *Principles of Surface Enhanced Raman Spectroscopy and Related Plasmonic Effects*, Elsevier, Amsterdam, 2009.
2 R. F. Aroca, *Surface-Enhanced Vibrational Spectroscopy*, John Wiley & Sons, Chichester, 2006.
3 J. Jiang, K. Bosnick, M. Maillard and L. Brus, *J. Phys. Chem. B*, 2003, **107**, 9964–9972.
4 T. O. Shegai and G. Haran, *J. Phys. Chem. B*, 2006, **110**, 2459–2461.
5 M. Moskovits, *J. Chem. Phys.*, 1982, **77**, 4408–4416.
6 E. C. Le Ru, M. Meyer, E. Blackie and P. G. Etchegoin, *J. Raman Spectrosc.*, 2008, **39**, 1127.
7 M. Osawa, N. Matsuda, K. Yoshii and I. Uchida, *J. Phys. Chem.*, 1994, **98**, 12702.
8 M. Moskovits and J. S. Suh, *J. Chem. Phys.*, 1982, **77**, 4408–4416.
9 M. Moskovits and J. S. Suh, *J. Phys. Chem.*, 1988, **92**, 6327–6329.
10 E. C. Le Ru, *et al.*, *Curr. Appl. Phys.*, 2008, **8**, 467–470.
11 S. Buchanan, E. C. Le Ru and P. G. Etchegoin, *Phys. Chem. Chem. Phys.*, 2009, **11**, 7406.
12 N. Karsi, P. Lang, M. Chehimi, M. Delamar and G. Horowitz, *Langmuir*, 2006, **22**, 3118–3124.
13 J. D. Jackson, *Classical Electrodynamics*, Wiley, New York, 2nd edn, 1998.
14 L. D. Landau, E. M. Lifshitz and L. P. Pitaevski, *Electrodynamics of Continous Media*, Elsevier, Amsterdam, 2nd edn, 2004.
15 E. C. Le Ru and P. G. Etchegoin, *Chem. Phys. Lett.*, 2006, **423**, 63.
16 E. C. Le Ru, *et al.*, *J. Phys. Chem. C*, 2008, **112**, 8117–8121.

Supplementary information for "Experimental demonstration of surface selection rules for SERS on flat metallic surfaces"

E. C. Le Ru, S. A. Meyer, C. Artur, P. G. Etchegoin, J. Grand, Philippe, and F. Maurel

S.I. SAMPLE PREPARATION AND MEASUREMENT

A gold film (45 nm thickness evaporated on glass with an intermediate 2 nm titanium adhesion layer) was immersed in a 1 μM Nile Blue (NB) solution in water for $\sim$ 30 min and then thoroughly washed with ultrapure water and dried. Films prepared with this method achieve a monolayer deposition on the surface (corroborated by independent electrochemical measurements) and present a good overall uniformity of the SERS signal at different positions. The Raman measurements have been carried out in a Jobin-Yvon LabRam spectrometer equipped with an Olympus BX41 microscope and a notch filter for 633 nm laser excitation. Polarisation elements ($\lambda/2$-waveplate and polarisers) are used to set the incoming and outgoing polarisation directions. The Au film sample is mounted in a motorised rotation stage (Thorlabs) that allows precise angular scans to be performed. Several points in the sample are measured at each angle, to ensure the results are not influenced by outliers.

S.II. ESTIMATION OF THE SERS EF

It is instructive to estimate, at least semi-quantitatively, the SERS EF corresponding to our measurements on a flat gold metallic surface. We focus here on the specific example of the spectrum of Fig. 1(b) of the main text. To this end, we first assume that the non-SERS differential Raman cross-section ($d\sigma/d\Omega$) of the Raman peaks of NB at 633 nm is of the order of $\sim 10^{-24}$ cm^2/sr; a typical value for dyes at resonance.[1] Secondly, the number of NB molecules in the spot can be estimated from the expected coverage[2] (5.5×10^{-11} mol/cm^2). Thirdly, we calibrated the absolute response of our system using a $\times$50 (NA=0.5) objective by characterizing its scattering volume as in Ref. 3, and measuring the Raman signal of N_2 (of known Raman differential cross-section[4]) in air. Putting these numbers together, we estimate a SERS enhancement factor of the order of only ≈ 0.1 for the spectrum of Fig. 1(b) of the main manuscript. Although a rough estimate, this figure is comparable to the value (≈ 0.06) predicted from theory. The remarkable point here is that we can observe a monolayer of molecules on a surface where the Raman signal is actually being quenched, rather than enhanced.

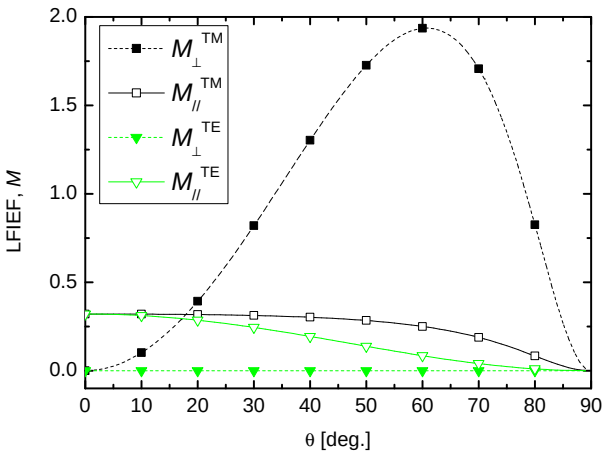

FIG. S1: Angular dependence of the Local Field Intensity Enhancement Factors (LFIEF, see Eqs. S1,S2) for the perpendicular (dashed lines, full symbols) and parallel (solid lines, hollow symbols) components of the electric field, excited with a TE- (triangles) or TM- (squares) polarized plane wave.

S.III. THEORETICAL PREDICTIONS

A. Layout of the problem

The Raman/SERS intensity or enhancement factor can be calculated from the standard theory of SERS[4] and from EM calculations for plane waves incident on a planar multilayer interface.[5] A brief account of the main principles is given in the following. For completeness, calculations were carried out on a layered structure that matches our gold film samples including all intermediate layers (for example, the titanium adhesion layer to the glass substrate). Plane waves with unit electric field amplitude are incident (with angle of incidence θ from the normal) from air ($n = 1$) onto a multilayer composed of:

- a 45 nm thick Au film, whose dielectric function is obtained from a fit of experimental data to a Drude[6,7] model with two critical points[4,8];
- a 2 nm titanium adhesion layer with dielectric function $\epsilon = -3.918 + 12.596i$ at 633 nm and $\epsilon = -4.031 + 13.48i$ at 658 nm (the Raman wavelength for the 590 cm^{-1} mode of NB);
- a semi-infinite glass ($n = 1.52$) medium (the substrate).

Because of the relatively thick Au layer (compared to the skin depth), the results are in fact very similar to those obtained for a simple air/gold interface.

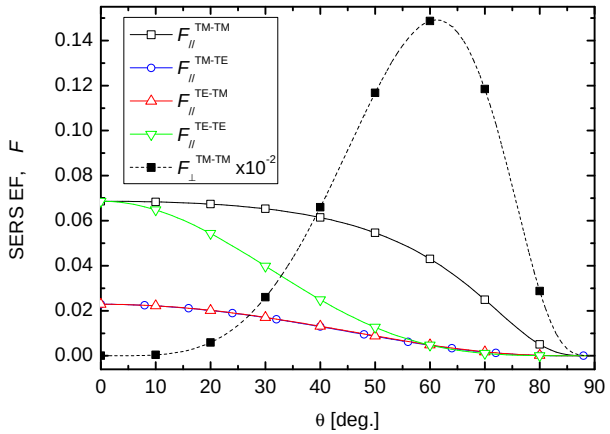

FIG. S2: Angular dependence of the SERS enhancement factors (F, see Eqs. S4,S5) for the 590 cm^{-1} NB Raman mode for the four excitation-detection polarizations (TM-TM: squares, TM-TE: circles, TE-TM: up triangles, TE-TE: down triangles), and two different uniaxial Raman tensors: in-plane (hollow symbols, solid lines) and out-of-plane (full symbols, dashed line).

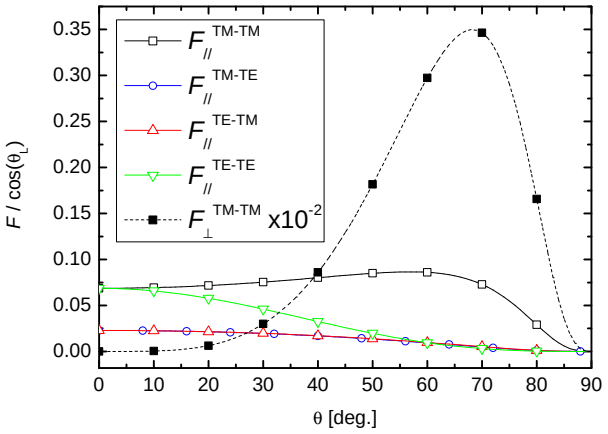

FIG. S3: SERS EF, F, as in Fig. S2, but including the geometrical correction for the excitation shape, i.e. $F/\cos(\theta_L)$.

B. Preliminary calculations

Calculations of the local electric field in this multilayer structure are performed using the SPlaC codes[9] as detailed in appendix F of Ref. 4. The local electric field $\mathbf{E}^{\mathrm{TM}}_{\mathrm{Loc}}(\lambda,\theta)$ and $\mathbf{E}^{\mathrm{TE}}_{\mathrm{Loc}}(\lambda,\theta)$ is calculated at the air/gold interface (on the air side) as a function of wavelength λ and angle θ for both TM and TE polarizations. Most of the properties of interest can then be derived from the local field intensity enhancement factors (LFIEFs) corresponding to the perpendicular and parallel components of the field, namely (with P=TM or TE, and $\mathbf{e}_z$ a unit vector normal to the interface):

$$M^P_\perp = \left|\mathbf{E}^P_{\mathrm{Loc}}\cdot\mathbf{e}_z\right|^2 \qquad \text{(S1)}$$

and

$$M^P_\parallel = \left|\mathbf{E}^P_{\mathrm{Loc}}\cdot\mathbf{e}_x\right|^2 + \left|\mathbf{E}^P_{\mathrm{Loc}}\cdot\mathbf{e}_y\right|^2 \qquad \text{(S2)}$$

Examples of the angular dependence of these quantities are given in Fig. S1. We note that $M^{\mathrm{TE}}_\perp = 0$ in this problem. We now briefly describe how these relate to the measured SERS intensities.

C. Prediction of SERS enhancement factors

For excitation at a given incident polarization P_L (P_L=TM or TE), incident angle θ_L, incident wavelength λ_L, and for a given Raman polarizability tensor $\hat{\alpha}$, the induced Raman dipole is $\mathbf{p} = \hat{\alpha}\cdot\mathbf{E}^{P_L}_{\mathrm{Loc}}(\lambda_L,\theta_L)$, and it is the emission of this dipole (modified by the presence of the metal) that we detect as a SERS signal at the Raman-shifted wavelength λ_R. This modified emission in a given direction θ_R can be deduced without further calculations using the optical reciprocity theorem.[4,10,11] If we analyze the emitted light along a given polarization P_R (P_R=TM or TE), the SERS enhancement factor can then be expressed as (see Sec. 4.5 of Ref. 4):

$$F^{P_L-P_R} = \left|\mathbf{E}^{P_R}_{\mathrm{Loc}}(\lambda_R,\theta_R)\cdot\hat{\alpha}_N\cdot\mathbf{E}^{P_L}_{\mathrm{Loc}}(\lambda_L,\theta_L)\right|^2. \qquad \text{(S3)}$$

where $\hat{\alpha}_N$ is the normalized Raman polarizability tensor.[3,4,12] Four such SERS EFs can be calculated (and measured) depending on the excitation-detection polarizations, i.e.: P_L and P_R being either TM or TE.

For a general $\hat{\alpha}_N$ this expression can be fairly complicated, so it is interesting to consider a few specific cases:

- For a uniaxial tensor with axis perpendicular to the plane, all tensor components are zero except[12] $\alpha_{Nzz} = \sqrt{15/4}$. In this case, we have:

  $$F^{P_L-P_R} = \frac{15}{4}M^{P_L}_\perp(\lambda_L,\theta_L)M^{P_R}_\perp(\lambda_R,\theta_R). \qquad \text{(S4)}$$

  As a result, we see that $F^{\mathrm{TE-TM}} = F^{\mathrm{TM-TE}} = F^{\mathrm{TE-TE}} = 0$ in this particular case.

- For a uniaxial tensor with axis parallel to the metallic plane, this axis may take any random orientation inside this plane ($\alpha_{Nxx} = \sqrt{15/4}$ only is an example, but $\alpha_{Nyy} = \sqrt{15/4}$ only is another one). Assuming a random in-plane orientation of this axis, we obtain after averaging:

  $$F^{P_L-P_R} = \frac{15}{4}\kappa^{P_L-P_R}M^{P_L}_\parallel(\lambda_L,\theta_L)M^{P_R}_\parallel(\lambda_R,\theta_R), \qquad \text{(S5)}$$

  where $\kappa^{P_L-P_R}$ results from the averaging process and is 1/5 for TM-TM and TE-TE, but 1/15 for TM-TE and TE-TM.

For our problem of interest here, we may assume in a first approximation that $\theta_R = \theta_L$ (i.e. backscattering

configuration) and take $\lambda_L = 633\,\text{nm}$ and $\lambda_R = 658\,\text{nm}$ (corresponding to the $590\,\text{cm}^{-1}$ of NB). The resulting predicted SERS EF for the four polarization configurations, and in the two extreme cases of out-of-plane and in-plane uniaxial tensors, are shown in Fig. S2. It is clear from these predictions that even a small α_{zz} component in the Raman tensor will strongly dominate the TM-TM signal, but should not contribute to the other three configurations.

D. Prediction of SERS intensities in the angle-dependent experiments

In order to predict the angular dependence of the SERS signal as measured in the experiments, we are now only lacking two ingredients:

- Firstly, the calculations of the SERS EFs do not take into account the geometrical shape of our incident beam. Thanks to the back-focal plane lens, the beam is to a very good approximation collimated, i.e. it contains only one incident angle θ_L. However, the size of the illuminated area on the sample changes with incident angle, and this affects the number of molecules in the beam. It should be noted that the power density felt by these molecules is the same, but there are just more of them contributing to the signal. This introduces an additional geometrical factor $1/\cos(\theta_L)$ in the measured SERS signal. Predictions including this correction are shown in Fig. S3.
- Secondly, since we use a microscope objective ($\times 20$, NA=0.35) to collect the emitted light, we are in reality collecting Raman light over a range of θ_R close to θ_L. This effect is secondary but can be accounted for by averaging the SERS EF over all possible θ_R that fall within the numerical aperture of the objective. This additional correction, although small, was applied to obtain the theoretical results shown in Fig. 2 of the main text, and for the fits of Fig. 3.

S.IV. EXPERIMENTAL DATA FOR THE 1645 CM^{-1} PEAK OF NILE BLUE

Fig. S4 is the equivalent of Fig. 3 of the main text, but for the $1645\,\text{cm}^{-1}$ peak of Nile Blue. The results are similar, although the data are subject to more uncertainties because the signal to noise ratio in this region of the spectrum is worse.

S.V. INFRARED ABSORPTION AND DFT STUDY OF THE ORIENTATION OF NB ON AU

PM-IRRAS spectra were recorded with a Nicolet 860 FTIR (Thermo- Electron) spectrometer with a resolution

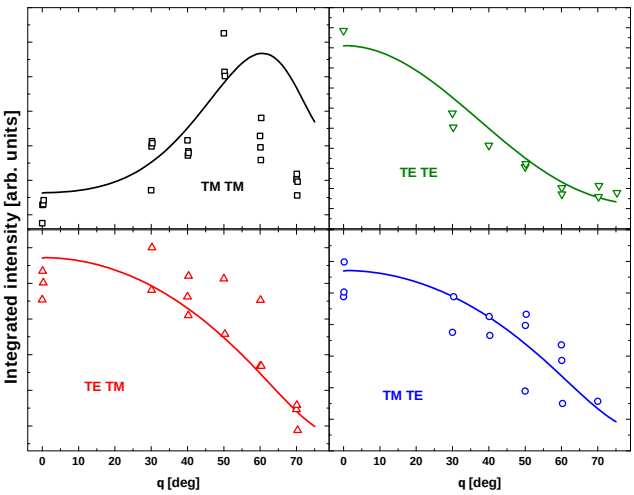

FIG. S4: Same as Fig. 3 of the main paper but for the $1645\,\text{cm}^{-1}$ peak of Nile Blue.

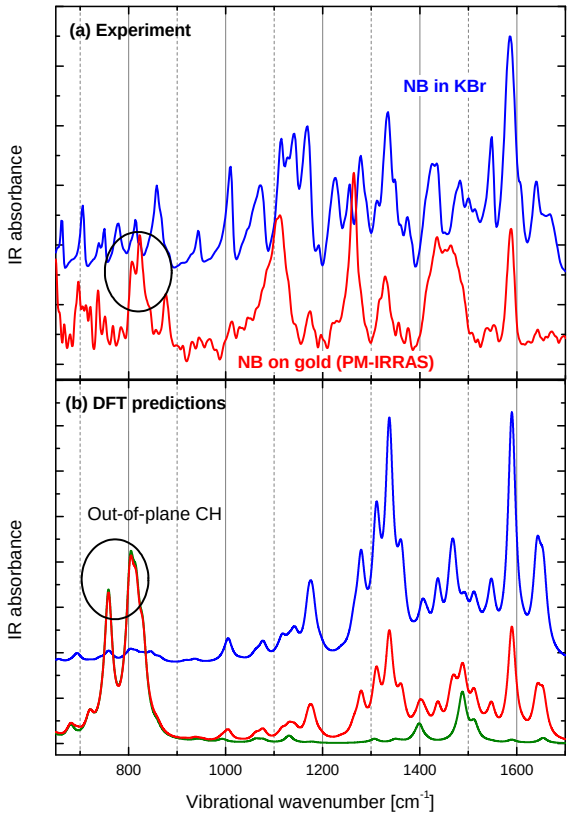

FIG. S5: (a) Experimental IR absorption of NB in KBr powder and PM-IRRAS of NB adsorbed on gold. (b) DFT predictions of the IR absorption of NB in the standard case (blue), for PM-IRRAS of NB adsorbed perfectly flat on a surface (green), and same with a small contribution of in-plane components (red). The out-of-plane CH bending modes are clearly visible in PM-IRRAS, indicating a majority of flat molecules.

of $8\,\mathrm{cm}^{-1}$ by adding 2000 scans with an optical mirror velocity of 0.474 cm-1/s. The spectrometer was equipped with a commercially available module (Thermo Electron) including a ZnSe photoelastic modulator (PEM) and measurements were performed at an incident angle of 80◦ under a (partially) dry atmosphere. After reflection on the sample, the incident beam is focused with a ZnSe lens on a MCT-A detector cooled at 77 K. The PEM oscillates at a frequency of 50 kHz and changes the polarization of the incident beam from parallel to perpendicular to the plane of incidence at a frequency of 100 kHz. The polarization-modulated signal is separated from the low frequency signal (between 380 and 3800 Hz) with a 48 kHz high-pass filter (GWC) and then demodulated. The two interferograms are high pass- and low pass-filtered by the spectrometer and simultaneously sampled by the dual-channel electronics. With the PM-IRRAS technique, the output signal is not directly proportional to the IR absorbance, but the quantity $(R_p-R_s)/(R_p+R_s)$ multiplied by a Bessel function that results from the Fourier transform of the doubly modulated input signal (R_p and R_s are the reflection coefficients for the p (TM) and s (TE) polarization, respectively). This background Bessel function varies slowly vs the wavenumber within a $20\,\mathrm{cm}^{-1}$ range (i.e. the width of an absorption peak). Then, the baseline was subtracted from a spline function of the spectrum excluding the vibrational absorptions. The resulting PM-IRRAS spectrum contains primarily the contribution of out-of-plane components of the IR dipoles.

The experimental PM-IRRAS spectrum of Nile Blue adsorbed on gold is shown in Fig. S5(a) (red curve) and compared to the bulk IR absorption of NB in KBr (blue curve). The marked difference in the prominent peaks indicate a preferred adsorption geometry. The new peaks appearing in the $800\,\mathrm{cm}^{-1}$ are in particular attributed to out-of-plane CH bending modes. We conclude that the NB molecules are adsorbed predominantly flat on the gold surface.

This interpretation is further backed up by Density Functional Theory (DFT) calculations of the NB molecule. DFT calculations were performed using the Gaussian DFT package[13] with Becke's 3-parameter hybrid functional[14] and Lee-Yang-Parr[15] non-local electron correlation (commonly abbreviated as B3LYP) with basis set 6-31G(d). A vibrational frequency analysis, which includes IR intensity (I) calculations, was carried out. IR dipoles, $\mathbf{p}$, were then derived from the normal mode displacements and the dipole derivatives. A scaling factor of 0.97 was used for the vibrational frequencies. The IR spectrum (blue curve in Fig .S5(b)) was obtained by plotting each mode as a Lorentzian with full width at half maximum of $20\,\mathrm{cm}^{-1}$ and integrated intensity I. The PM-IRRAS spectrum of NB adsorbed perfectly flat on a surface (green cruve) was obtained by changing the IR intensities to $I \times |p_z|^2/|\mathbf{p}|^2$. For the second PM-IRRAS spectrum (red curve), the IR intensities were changed to: $I \times \left[0.97|p_z|^2/|\mathbf{p}|^2 + 0.03(|p_x|^2 + |p_y|^2)/|\mathbf{p}|^2\right]$, to qualitatively represent a predominantly flat adsorption geometry with small imperfections.

[1] S. A. Meyer, E. C. Le Ru, and P. G. Etchegoin, J. Phys. Chem. A **114**, 5515 (2010).
[2] H. Kuramitz, K. Sugawara, M. Kawasaki, K. Hasebe, H. Nakamura, and S. Tanaka, Anal. Sci. **15**, 589 (1999).
[3] E. C. Le Ru, E. Blackie, M. Meyer, and P. G. Etchegoin, J. Phys. Chem. C **111**, 13794 (2007).
[4] E. C. Le Ru and P. G. Etchegoin, *Principles of Surface Enhanced Raman Spectroscopy and Related Plasmonic Effects* (Elsevier, Amsterdam, 2009).
[5] J. D. Jackson, *Classical electrodynamics* (Wiley, New York, 1998), 2nd ed.
[6] P. Drude, Annalen der Physik **306**, 566 (1900).
[7] P. Drude, Annalen der Physik **308**, 369 (1900).
[8] P. G. Etchegoin, E. C. Le Ru, and M. Meyer, J. Chem. Phys. **125**, 164705 (2006).
[9] These Matlab codes are part of the SPlaC package, which can be downloaded from http://www.victoria.ac.nz/raman/book/codes.aspx.
[10] E. C. Le Ru and P. G. Etchegoin, Chem. Phys. Lett. **423**, 63 (2006).
[11] E. C. Le Ru, J. Grand, N. Félidj, J. Aubard, G. Lévi, A. Hohenau, J. R. Krenn, E. Blackie, and P. G. Etchegoin, J. Phys. Chem. C **112**, 8117 (2008).
[12] E. C. Le Ru, M. Meyer, E. Blackie, and P. G. Etchegoin, J. Raman Spectrosc. **39**, 1127 (2008).
[13] M. J. Frisch, G. W. Trucks, H. B. Schlegel, G. E. Scuseria, M. A. Robb, J. R. Cheeseman, J. A. Montgomery, Jr., T. Vreven, K. N. Kudin, et al., Tech. Rep., Gaussian, Inc., Pittsburgh PA (2003).
[14] A. D. Becke, J. Chem. Phys. **98**, 5648 (1993).
[15] C. Lee, W. Yang, and R. G. Parr, Phys. Rev. B **37**, 785789 (1988).